




Original Article

Chemogenetic activation of astrocytes modulates sleep–wakefulness states in a brain region-dependent manner

Yuta Kurogi^{1,2}, Tomomi Sanagi³, Daisuke Ono^{4,5}  and Tomomi Tsunematsu^{2,3,*} 

¹Graduate School of Life Sciences, Tohoku University, Sendai, Japan,

²Department of Biological Sciences, Faculty of Science, Hokkaido University, Sapporo, Japan,

³Creative Interdisciplinary Research Division, Frontier Research Institute for Interdisciplinary Sciences, Tohoku University, Sendai, Japan,

⁴Stress Recognition and Response, Research Institute of Environmental Medicine, Nagoya University, Nagoya, Japan and

⁵Department of Neural Regulation, Nagoya University Graduate School of Medicine, Nagoya, Japan

*Corresponding author. Tomomi Tsunematsu, Department of Biology, Faculty of Science, Hokkaido University, Sapporo 060-0810, Japan, Email: tsune@sci.hokudai.ac.jp.

Abstract

Study Objectives: Astrocytes change their intracellular calcium (Ca^{2+}) concentration during sleep/wakefulness states in mice. Furthermore, the Ca^{2+} dynamics in astrocytes vary depending on the brain region. However, it remains unclear whether alterations in astrocyte activity can affect sleep–wake states and cortical oscillations in a brain region-dependent manner.

Methods: Astrocyte activity was artificially manipulated in mice using chemogenetics. Astrocytes in the hippocampus and pons, which are 2 brain regions previously classified into different clusters based on their Ca^{2+} dynamics during sleep–wakefulness, were focused on to compare whether there are differences in the effects of astrocytes from different brain regions.

Results: The chemogenetic activation of astrocytes in the hippocampus significantly decreased the total time of wakefulness and increased the total time of sleep. This had little effect on cortical oscillations in all sleep–wakefulness states. On the other hand, the activation of astrocytes in the pons substantially suppressed rapid eye movement (REM) sleep in association with a decreased number of REM episodes, indicating strong inhibition of REM onset. Regarding cortical oscillations, the delta wave component during non-REM sleep was significantly enhanced.

Conclusions: These results suggest that astrocytes modulate sleep–wakefulness states and cortical oscillations. Furthermore, the role of astrocytes in sleep–wakefulness states appears to vary among brain regions.


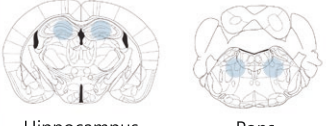
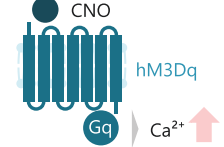
Submitted for publication: July 24, 2024; Revised: December 4, 2024

© The Author(s) 2024. Published by Oxford University Press on behalf of Sleep Research Society.

This is an Open Access article distributed under the terms of the Creative Commons Attribution-NonCommercial-NoDerivs licence (<http://creativecommons.org/licenses/by-nc-nd/4.0/>), which permits non-commercial reproduction and distribution of the work, in any medium, provided the original work is not altered or transformed in any way, and that the work properly cited. For commercial re-use, please contact reprints@oup.com for reprints and translation rights for reprints. All other permissions can be obtained through our RightsLink service via the Permissions link on the article page on our site—for further information please contact journals.permissions@oup.com.

Graphical Abstract

Chemogenetic activation of astrocytes modulates sleep/wakefulness states in a brain region-dependent manner

Background		Questions																						
<ul style="list-style-type: none"> ● Astrocyte Ca^{2+} concentration correlates with sleep/wakefulness states. ● Astrocyte Ca^{2+} dynamics differ between brain regions. (Tsunematsu et al., 2021, <i>J Neurosci.</i>) 		<ul style="list-style-type: none"> ● Does the activation of astrocytes affect sleep/wakefulness states? ● What would be the effect of activating astrocytes in different brain regions? 																						
Methods		Results & Conclusions																						
<p>Virus injection</p> <p>Expression of hM3Dq in astrocytes</p> <p>GFAP-cre mice</p> <p>AAV-CAG-FLEX-hM3Dq-mCherry</p>  <p>Target brain regions</p> <p>Hippocampus Pons</p>  <p>DREADD system</p>  <p>Schedule</p> <ul style="list-style-type: none"> Day0 Virus injection Day7 EEG/EMG electrode implantation Day17~ CNO/saline injection EEG/EMG recording 		<table border="1"> <thead> <tr> <th></th> <th>Hippocampus</th> <th>Pons</th> </tr> </thead> <tbody> <tr> <td>Sleep/wakefulness state</td> <td></td> <td></td> </tr> <tr> <td>Wake</td> <td>↓</td> <td>—</td> </tr> <tr> <td>NREM</td> <td>↑</td> <td>↑</td> </tr> <tr> <td>REM</td> <td>↑</td> <td>↓</td> </tr> <tr> <td>Cortical oscillation</td> <td></td> <td></td> </tr> <tr> <td>NREM δ wave</td> <td>—</td> <td>↑</td> </tr> </tbody> </table> <p>● Astrocytes can modulate sleep/wakefulness states.</p> <p>● The role of astrocytes in sleep/wakefulness regulation varies depending on the brain region.</p>			Hippocampus	Pons	Sleep/wakefulness state			Wake	↓	—	NREM	↑	↑	REM	↑	↓	Cortical oscillation			NREM δ wave	—	↑
	Hippocampus	Pons																						
Sleep/wakefulness state																								
Wake	↓	—																						
NREM	↑	↑																						
REM	↑	↓																						
Cortical oscillation																								
NREM δ wave	—	↑																						

Key words: astrocyte; REM sleep; NREM sleep; wakefulness; EEG; hippocampus; pons; chemogenetics

Statement of Significance

Sleep is an instinctive behavior for many organisms. Recently, it has been reported that not only neurons but also astrocytes, a type of glial cell, contribute to sleep–wakefulness states. Intracellular Ca^{2+} concentration, an indicator of astrocyte activity, fluctuates during sleep–wakefulness states. However, it is still unclear whether changes in astrocyte activity can affect sleep–wakefulness states. In this study, we utilized chemogenetics to activate astrocytes in mice. Our results showed that activation of astrocytes in the hippocampus causes decreased wakefulness and that in the pons causes decreased rapid eye movement sleep. Therefore, our findings demonstrate that the activation of astrocytes modulates sleep–wakefulness states in a brain region-dependent manner.

Astrocytes are one of the most abundant cell types in the brain. It is well known that astrocytes have housekeeping roles in brain function, contributing to ion buffering, neurotransmitter recycling, and metabolism regulation [1, 2]. As astrocytes are non-excitable, all of their physiological functions are strongly affected by the dynamics of their intracellular Ca^{2+} concentration. Recently, a growing body of evidence has indicated that astrocytes play a crucial role in the regulation and physiological functions of sleep [3]. Astrocytes release a variety of sleep-promoting chemicals, such as cytokines, neurotrophins, prostaglandins, and purines [4–8]. In addition, several studies, including ours, have reported that intracellular Ca^{2+} concentrations in astrocytes substantially fluctuate through sleep–wakefulness states [9–11]. The intracellular Ca^{2+} concentration of astrocytes is highest during wakefulness and lowest during sleep, although this degree varies depending on the brain region [11]. These results indicate that astrocytes in different brain regions have different functions in sleep–wakefulness states.

Previous studies have suggested that intracellular Ca^{2+} dynamics in astrocytes play a crucial role, particularly in the regulation of rapid eye movement (REM) sleep. A decrease in intracellular

Ca^{2+} concentrations in astrocytes occurs during sleep, and this decrease is more pronounced during REM sleep than during non-REM (NREM) sleep in the frontal cortex [9], barrel cortex [10, 11], hippocampus, hypothalamus, cerebellum, and pons [11]. The reduction of inositol 1,4,5-trisphosphate in astrocytes throughout the brain results in a constant suppression of Ca^{2+} release from intracellular Ca^{2+} stores and alters the duration and strength of theta waves during REM sleep [12].

In the present study, we focused on two brain regions that play important roles in REM sleep. The pons, which contains various neurons that are involved in the regulation of REM sleep [13–15], and the hippocampus, which generates theta waves, the electroencephalogram (EEG) characteristic of REM sleep [16, 17]. Moreover, in our previous study, we showed that astrocytes in the hippocampus and the pons are classified into various different clusters based on their intracellular Ca^{2+} dynamics during sleep–wakefulness states [11]. We, therefore, suspected that they might have different roles in sleep–wakefulness modulation. Therefore, in this study, we investigated whether artificially manipulating astrocyte activity affects sleep–wakefulness states and cortical oscillations in mice. To answer these questions, we utilized

a chemogenetics approach. Our results showed that the activation of astrocytes in the hippocampus decreased wakefulness and increased sleep. On the other hand, the activation of astrocytes in the pons substantially suppressed REM sleep. In addition, the delta wave component of the EEG during NREM sleep was enhanced. These results suggest that astrocyte activity regulates sleep–wakefulness states and that different brain regions play different roles in sleep–wakefulness regulation.

Methods

Mice

All experimental procedures involving mice were approved by the Animal Care and Use Committee of Tohoku University (study approval no.: 2019LSA-018) and Hokkaido University (study approval no.: 23-0117), and were conducted in accordance with the National Institute of Health guidelines. All efforts were made to minimize animal suffering and discomfort and to reduce the number of animals used. Mice were housed under a controlled 12–12 h light–dark cycle (light on hours: 8:00–20:00). Mice had ad libitum access to food and water. Glial fibrillary acidic protein (GFAP)-cre mice on a C57BL/6J background (024098, The Jackson Laboratory) were used to chemogenetically manipulate the activity of astrocytes. The following polymerase chain reaction (PCR) primer sets were used for mouse genotyping: GFAPcre Fw (5'-TCCATAAAGGCCCTGACATC-3') and GFAPcre Rv (5'-TGCGAACCTCATCACTCGT-3'). A total of 22 male GFAP-cre mice were used. For chemogenetics experiments, 12 mice were used. For cFos immunohistochemistry studies, 10 mice were used. In this study, female mice were not used, because the sleep pattern of female mice on the C57 genetic background has been reported to be affected by the estrous cycle [18].

Viruses

Adeno-associated viruses were generated using a triple-transfection, helper-free method, and purified following previously established procedures [19]. In brief, human embryonic kidney 293A cells (Invitrogen) were transfected with pHelper, pAAV5, and pAAV-CAG-FLEX-hM3Dq-mCherry using the standard calcium phosphate method. Three days after transfection, the cells were collected and suspended in phosphate buffer saline (PBS) containing 1 mM MgCl₂. After two freeze-thaw cycles, the cell lysate was treated with benzonase nuclease (Merck) at 37°C for 30 minutes, followed by centrifugation twice at 15 000 g for 10 minutes each. The supernatant containing the viruses was collected for further use. The titer of the AAV vector was determined by quantitative PCR: AAV₅-CAG-FLEX-hM3Dq-mCherry, 2×10^{12} . The final purified viruses were stored at –80°C.

Surgical procedures

Male GFAP-cre mice approximately three to six months old were used (111.7 ± 6.3 days of age). Stereotaxic surgery was performed under anesthesia with pentobarbital (5 mg/kg, intraperitoneal [i.p.] injection as induction) and with isoflurane (1%–2% for maintenance) using a vaporizer for small animals (Bio Research Center), with the mice positioned in a stereotaxic frame (Narishige). For chemogenetics experiments, AAV₅-CAG-FLEX-hM3Dq-mCherry was bilaterally injected into the dentate gyrus of the hippocampus (1.7 mm posterior, ± 0.8 mm lateral, and a depth of 2.0 mm from bregma), or the sublateralodorsal tegmental nucleus (SLD) of the pons (5.3 mm posterior, ± 1.0 mm lateral, and a depth of 4.0 mm from bregma) of GFAP-cre mice in a volume of 200 nL and

at a flow rate of 20 nL per min using a Hamilton 10 µL syringe. The needle was kept in place for 10 minutes after the injection. The injection volume and flow rate were controlled by a stereotaxic injector (Legato 130, Muromachi Kikai). One week after the AAV injection, surgery for EEG/electromyogram (EMG) recordings were performed. Three screws were implanted into the skull, as electrodes for the measurement of cortical EEGs. The positions of the three electrodes were 1 mm anterior, 1 mm lateral (left), and 2.5 mm posterior, 2 mm lateral (right and left) for hippocampal experiments; 1 mm anterior, 1 mm lateral (left), and 1.5 mm posterior, 1 mm lateral (right and left) for pons experiments. Twisted wires (AS633, Cooner wire) were inserted into the neck muscle as electrodes for EMGs. Another bone screw was implanted into the cerebellum as a ground. All electrodes were connected to a pin socket and fixed to the skull with dental cement. After the surgery, the mice were left to recover for at least 7 days and then transferred to sleep recording chambers.

Chemogenetics

Clozapine N-oxide (CNO; ab141704, Abcam) was dissolved in saline to 1 mg/mL. CNO or saline was administered by i.p. injection to each mouse (0.3 mL/30 g body weight) at Zeitgeber time 1. Each mouse received three saline and three CNO administrations in a random manner, at intervals of 3 days. The results obtained from three repetitions were averaged, and treated as the data for one mouse.

In vivo sleep–wakefulness recording using freely moving mice

Continuous EEG and EMG recordings were conducted through a slip ring (SPM-35-8P-03, HIKARI DENSHI), which was designed so that the movement of the mice was unrestricted. Two of the three screw electrodes were used for the EEG recordings. Differential amplification was performed for the EEG and EMG signals (AB-610J, Nihon Koden). Amplified signals were then filtered (EEG, 0.75–20 Hz; EMG, 20–50 Hz), digitized at a sampling rate of 128 Hz, and recorded using SleepSign software version 3 (Kissei Comtec). Mouse behavior was monitored through a charge-coupled device video camera and recorded on a computer synchronized with EEG and EMG recordings using the SleepSign video option system (Kissei Comtec).

Immunohistochemistry

To confirm the specific expression of hM3Dq in astrocytes, mice were deeply anesthetized with isoflurane, and perfused sequentially with 20 mL of chilled PBS and 20 mL of chilled 4% paraformaldehyde in PBS (Nacalai Tesque). To confirm the activation of astrocytes via CNO, mice were deeply anesthetized 90 minutes after CNO or saline injection and perfused in a similar way. The brains were removed and immersed in the above fixation solution overnight at 4°C, and then immersed in 30% sucrose in PBS for at least 2 days. The brains were quickly frozen in embedding solution (Sakura Finetek), and cut into coronal sections using a cryostat (CM1850 or CM3050S, Leica) at a thickness of 40 µm. For astrocyte immunostaining, brain sections were incubated with an anti-GFAP antibody (1:2,000; G3893, Sigma) overnight at 4°C. Then, the sections were incubated with CF488A donkey anti-mouse immunoglobulin G (IgG) (1:1000; 20014-1, Nacalai Tesque) for 2 hours at room temperature. To confirm the specificity of the antibodies, incubations without the primary antibody were conducted as a negative control, and no signal was observed. For microglia immunostaining, sections were incubated with an

anti-ionized calcium-binding adapter protein 1 (Iba1) antibody (1:1000; 019-19741, FUJIFILM Wako Pure Chemical) overnight at 4°C. Then, the sections were incubated with CF488A donkey anti-rabbit IgG (1:1000; 20015-1, Nacalai Tesque) for 2 hours at room temperature. To visualize neurons, Nissl staining was performed. The brain sections were incubated with NeuroTrace Green Fluorescent Nissl Stain (1:300; N21480, Invitrogen) for one hour at room temperature. Regarding cFos immunostaining, to confirm the activation effect of hM3Dq on astrocytes, CNO was administrated intraperitoneally 90 minutes before perfusion. Brain sections were incubated with an anti-cFos antibody (1:5000; 226008, Synaptic Systems GmbH) overnight at 4°C. Then, the sections were incubated with CF488A donkey anti-rabbit IgG (1:1000; 20015-1, Nacalai Tesque) for 2 hours at room temperature. All sections were incubated with 4',6-diamidino-2-phenylindole (DAPI) (1:1000; D523, Dojindo) for 30 minutes at room temperature to visualize nuclei. The sections were mounted onto APS-coated slides, coverslipped with 50% glycerol in PBS, and observed using a fluorescence microscope (BZ-X800L or BZ-9000, Keyence).

To quantify the activation effect of hM3Dq on astrocytes by the i.p. injection of CNO, image analysis was performed using ImageJ software (version 1.54f). For each mouse, three regions of interest (ROIs) (90 × 120 μm) were selected from the hippocampus across two or three brain sections, and three ROIs were selected from the pons across two or three brain sections. For hippocampal experiments, ROIs were selected 1.3–2.3 mm posterior, 0.2–2.1 mm lateral, and at a depth of 1.7–2.3 mm from bregma; for pons experiments, ROIs were selected 5.0–5.8 mm posterior, 0.6–1.5 mm lateral, and at a depth of 2.3–3.9 mm from bregma. For cFos quantification, a threshold was applied to the ROI using the ImageJ plugin adaptive threshold by Qingzong TSENG to binarize the image and calculate the area of hM3Dq-mCherry and colocalization area of hM3Dq-mCherry and cFos-positive (<https://sites.google.com/site/qingzongtseng/adaptivethreshold>). Then, the area of colocalization of hM3Dq-mCherry and cFos-positive was divided by the area of hM3Dq-mCherry. Results were compared between CNO-treated ($n = 3$) and saline-treated mice ($n = 3$).

Sleep scoring and EEG analysis

Polysomnographic recordings were automatically scored offline, with each epoch scored as wakefulness, NREM sleep, or REM sleep by SleepSign software (Kissei Comtec) in 4-second epochs, in accordance with standard criteria [20, 21]. All vigilance state classifications assigned by SleepSign were confirmed visually. The same individual, blinded to the experimental condition, scored all EEG/EMG recordings. Three consecutive 4-second epochs (12 seconds) had to be scored as a single state before being considered as a sleep or wake bout and were then used for subsequent analysis. Spectral analysis of the EEGs was performed by Fast Fourier transform, which yielded a power spectral profile with a 1-Hz resolution divided into delta (1–5 Hz), theta (6–10 Hz), alpha (10–13 Hz), and beta (13–20 Hz) waves. The EEG spectral power was normalized in the following way. EEGs from mice during the 4-hour period after CNO or saline injection were averaged in 1-Hz bins for each of wakefulness, NREM sleep, and REM sleep. Then, each of the averages in 1-Hz bins was divided by the total of the average values from 0.75 to 20 Hz for each of wakefulness, NREM sleep, and REM sleep, respectively. To calculate the EEG power of the delta, theta, alpha, and beta bands for each sleep–wakefulness state, the EEG values from 1–5 Hz, 6–10 Hz, 10–13 Hz, and 13–20 Hz were summed, respectively. Each summed value was

then divided by the total average value from 0.75 to 20 Hz for wakefulness, NREM sleep, and REM sleep. Saline data were normalized by the total values of the saline treatment, and CNO data were normalized by the total values of the CNO treatment.

Statistical Analysis

Data are presented as the mean ± standard error of the mean (SEM) unless otherwise stated. Statistical analyses were performed using MATLAB software (MathWorks). For the data of hourly time-in-state and normalized EEG power, a repeated measures Analysis of variance (ANOVA) with the post hoc Tukey criterion was performed. Other data were analyzed by the paired t-test. A p -value of less than .05 was considered to indicate a statistically significant difference between groups.

Results

Specific expression of hM3Dq in hippocampal astrocytes

To study the role of hippocampal astrocytes in sleep–wakefulness regulation, we introduced a designer receptor exclusively activated by a designer drug (DREADD) in astrocytes. To enhance the activity of astrocytes, we bilaterally injected the excitatory chemogenetic virus AAV-CAG-FLEX-hM3Dq-mCherry into the hippocampus of GFAP-cre mice (Figure 1A). The specific expression of hM3Dq in astrocytes was confirmed by immunohistochemical staining using the astrocyte-specific marker GFAP. The merged images show that hM3Dq-mCherry was exclusively observed in hippocampal astrocytes (Figure 1B). Iba1 staining for microglia, and NeuroTrace green fluorescent Nissl staining for neurons showed no staining of the hM3Dq-mCherry-positive cells (Figure 1, C and D). A previous study using the same Nissl staining solution showed that staining was not observed in astrocytes, microglia, and oligodendrocytes [22], indicating no aberrant staining. The area of virus infection and the total time in the sleep/wakefulness state of each mouse are shown in Supplementary Figure S1.

Chemogenetic activation of hippocampal astrocytes decreases wakefulness and increases sleep

First, to confirm whether the i.p. administration of CNO (1 mg/kg) induces the activation of astrocytes, we performed immunostaining of cFos, which is an immediately early gene, as a marker of cellular activation. The mice were injected with CNO or saline, and their brains were collected after 90 minutes. Immunohistochemical analyses demonstrated that the mice with chemogenetic activation of astrocytes had significantly increased cFos expression in the hippocampus compared with saline-treated control mice ($t(2) = 7.24$, $p < .05$, paired t-test; Figure 2, A and B).

To determine the sleep–wakefulness states of mice during chemogenetic activation of hippocampal astrocytes, mice were chronically implanted with EEG and EMG electrodes in freely moving conditions. GFAP-cre mice expressing hM3Dq specifically in hippocampal astrocytes were injected i.p. with CNO (1 mg/kg) or with saline as a control at ZT1 ($n = 6$), and their hourly amount of sleep–wakefulness was analyzed (Figure 2, C, G, and K, and Supplementary Table S1). Although the hourly amounts of sleep–wakefulness states for 24 hours showed no significant change, during the 4 hours post-injection period (from ZT1 to

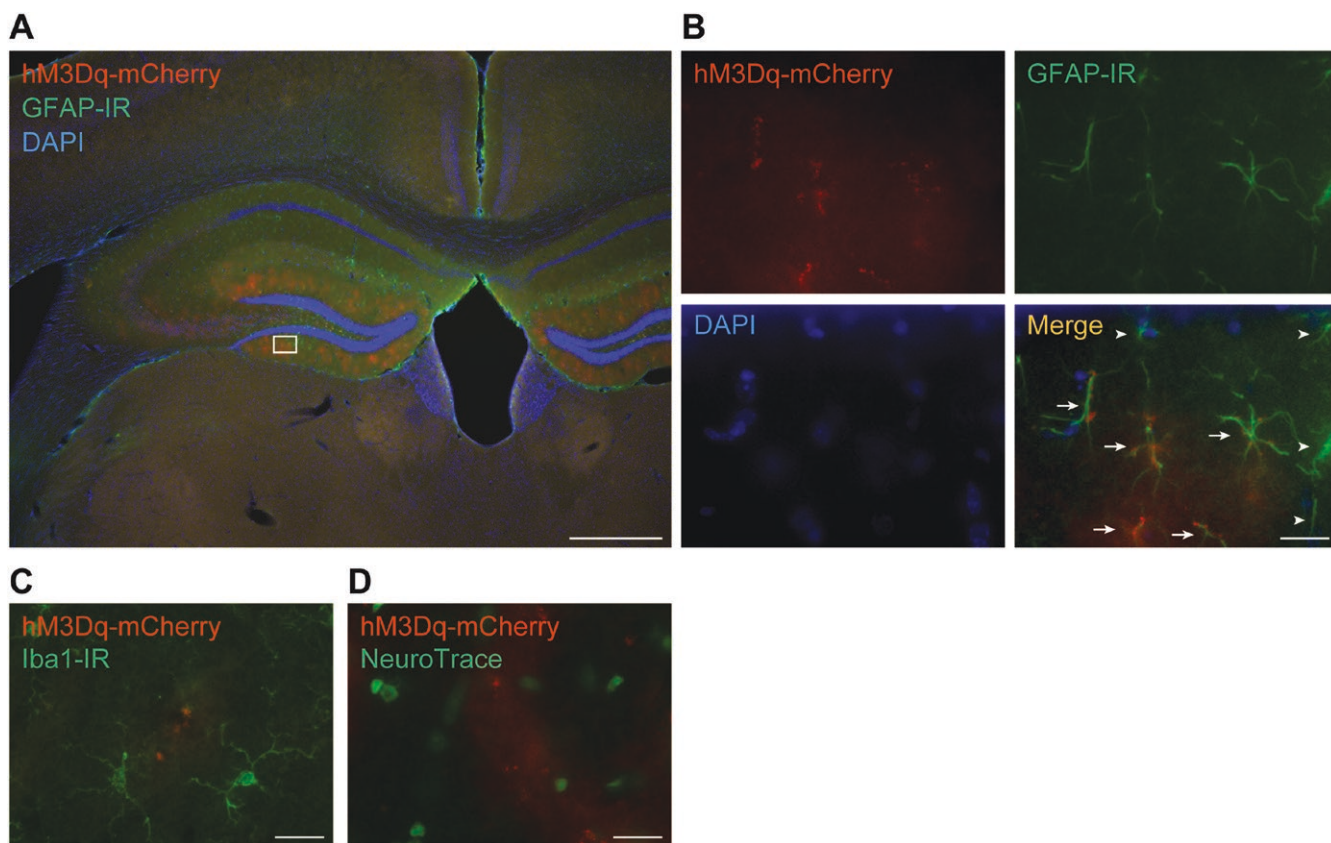


Figure 1. Specific expression of hM3Dq in hippocampal astrocytes. (A) Expression pattern of hM3Dq in the hippocampus of GFAP-cre mice. Red, hM3Dq-mCherry; green, GFAP-IR astrocytes; blue, DAPI. Scale bar: 500 μ m. (B) Higher magnifications of the square region in (A). Arrows indicate GFAP-immunoreactive (IR) astrocytes expressing hM3Dq. Arrowheads indicate GFAP-IR astrocytes not expressing hM3Dq. Scale bar: 10 μ m. (C) Fluorescence immunostaining using an anti-Iba1 antibody. Red, hM3Dq-mCherry; green, Iba1-IR microglia. Scale bar: 10 μ m. (D) NeuroTrace green fluorescent Nissl staining. Red, hM3Dq-mCherry; green, NeuroTrace green fluorescent Nissl stain-positive neurons. Scale bar: 10 μ m.

ZT4), the total time of wakefulness significantly decreased ($t(5) = -5.03$, $p < .01$, paired t -test; [Figure 2D](#)). In contrast, the total time of NREM sleep and REM sleep significantly increased (NREM sleep: $t(5) = 2.93$, $p < .05$, paired t -test; REM sleep: $t(5) = 2.61$, $p < .05$, paired t -test; [Figure 2, H and L](#)). There was a significant increase in the mean episode duration of NREM sleep ($t(5) = 4.24$, $p < .01$, paired t -test; [Figure 2I](#)), but not for wakefulness or REM sleep ([Figure 2, E and M](#)). There were no significant changes in the number of episodes across all sleep-wakefulness states ([Figure 2, F, J, and N](#)). Transition frequencies during all sleep-wakefulness states and in each state did not change in the 4-hour post-injection period ([Figure 2, O and P](#)). These results demonstrated that the activation of astrocytes in the hippocampus induces a decrease in wakefulness and an increase in sleep.

Hippocampal astrocyte activation has little effect on cortical oscillations

As the activation of hippocampal astrocytes caused changes in sleep-wakefulness states, we next analyzed cortical oscillations based on the EEG in each sleep-wakefulness state for 4 hours after CNO injection ($n = 6$). EEG power values in each 1-Hz bin were normalized for a total of 0.75 to 20 Hz EEG power during the 4-hour post-injection period in each of wakefulness, NREM sleep, and REM sleep ([Figure 3, A, C, and E](#), respectively). The activation of hippocampal astrocytes had no change in cortical oscillations during sleep-wakefulness ([Figure 3, A, C, and E](#) and [Supplementary Table S2](#)). We further analyzed the EEG in

frequency bands, with 1 to 5 Hz as delta waves, 6 to 10 Hz as theta waves, 10 to 13 Hz as alpha waves, and 13 to 20 Hz as beta waves ([Figure 3, B, D, and F](#)). No significant differences were found compared with saline-treated experiments. These results indicate that the activation of hippocampal astrocytes has little effect on the EEG during sleep-wakefulness states.

Specific expression of hM3Dq in pons astrocytes

Next, to study the role of pons astrocytes in sleep-wakefulness regulation, the activity of astrocytes was manipulated in the pons, similar to the experiments conducted in the hippocampus, using chemogenetics ([Figure 4A](#)). The specific expression of hM3Dq in astrocytes was confirmed by immunohistochemical staining of the astrocyte-specific marker GFAP. The merged images show that hM3Dq-mCherry was exclusively observed in pons astrocytes ([Figure 4B](#)). None of the microglia and neurons stained with Iba1 and NeuroTrace green fluorescent Nissl stain, respectively, were hM3Dq-mCherry-positive ([Figure 4, C and D](#), respectively), indicating the absence of ectopic expression. The area of virus infection, and the total time in the sleep-wakefulness state of each mouse are shown in [Supplementary Figure S2](#).

Chemogenetic activation of pons astrocytes substantially decreases REM sleep

cFos expression was analyzed immunohistochemically to determine whether the i.p. administration of CNO (1 mg/kg) induces the activation of astrocytes in the pons as well as in the

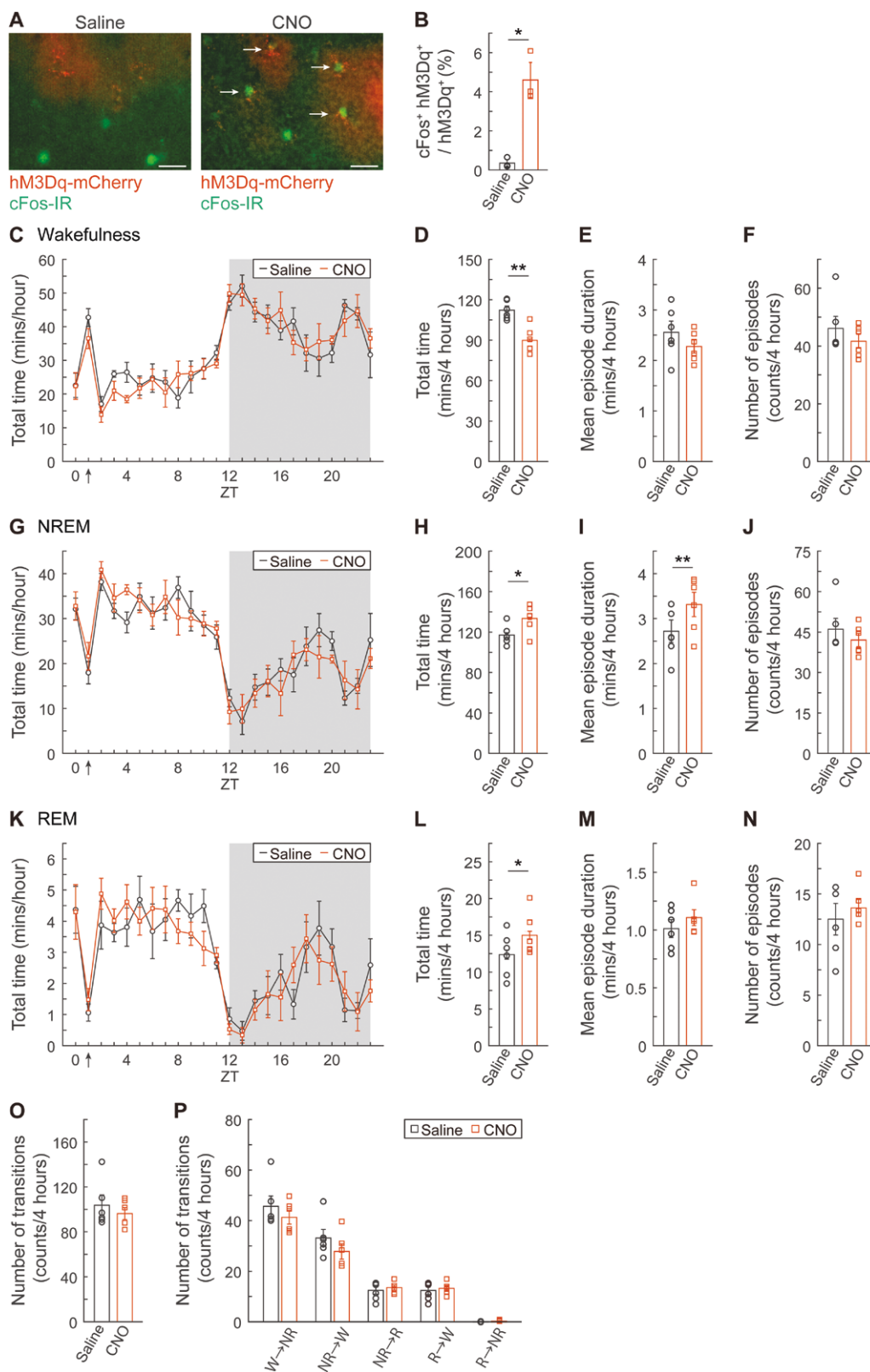


Figure 2. Effects of the chemogenetic activation of hippocampal astrocytes on sleep–wakefulness. (A) CNO administration (1 mg/kg) to mice expressing hM3Dq in their hippocampal astrocytes resulted in increased cFos expression (right) in the astrocytes (arrows) compared with saline-treated mice (left). Red, hM3Dq-mCherry; green, cFos-IR cells. Scale bar: 10 μ m. (B) Bar graph showing quantification results of c-Fos expression in the astrocytes. (C, G, and K) Hourly amounts of wakefulness (C), NREM sleep (G), and REM sleep (K) after i.p. injection of saline or CNO at ZT1 (arrows). The gray background indicates the dark period. (D, H, and L) Total amount of wakefulness (D), NREM sleep (H), and REM sleep (L) in the 4 hours after i.p. injection of saline or CNO. (E, I, and M) Mean episode duration of wakefulness (E), NREM sleep (I), and REM sleep (M). (F, J, and N) Number of episodes of wakefulness (F), NREM sleep (J), and REM sleep (N). (O) The number of transitions between all sleep–wakefulness states during the 4 hours after saline or CNO administration. (P) The number of transitions between sleep–wakefulness states during the 4 hours after saline or CNO administration. NR, NREM sleep; R, REM sleep; W, wakefulness. Values are represented as means \pm SEM; *, $p < .05$. **, $p < .01$.

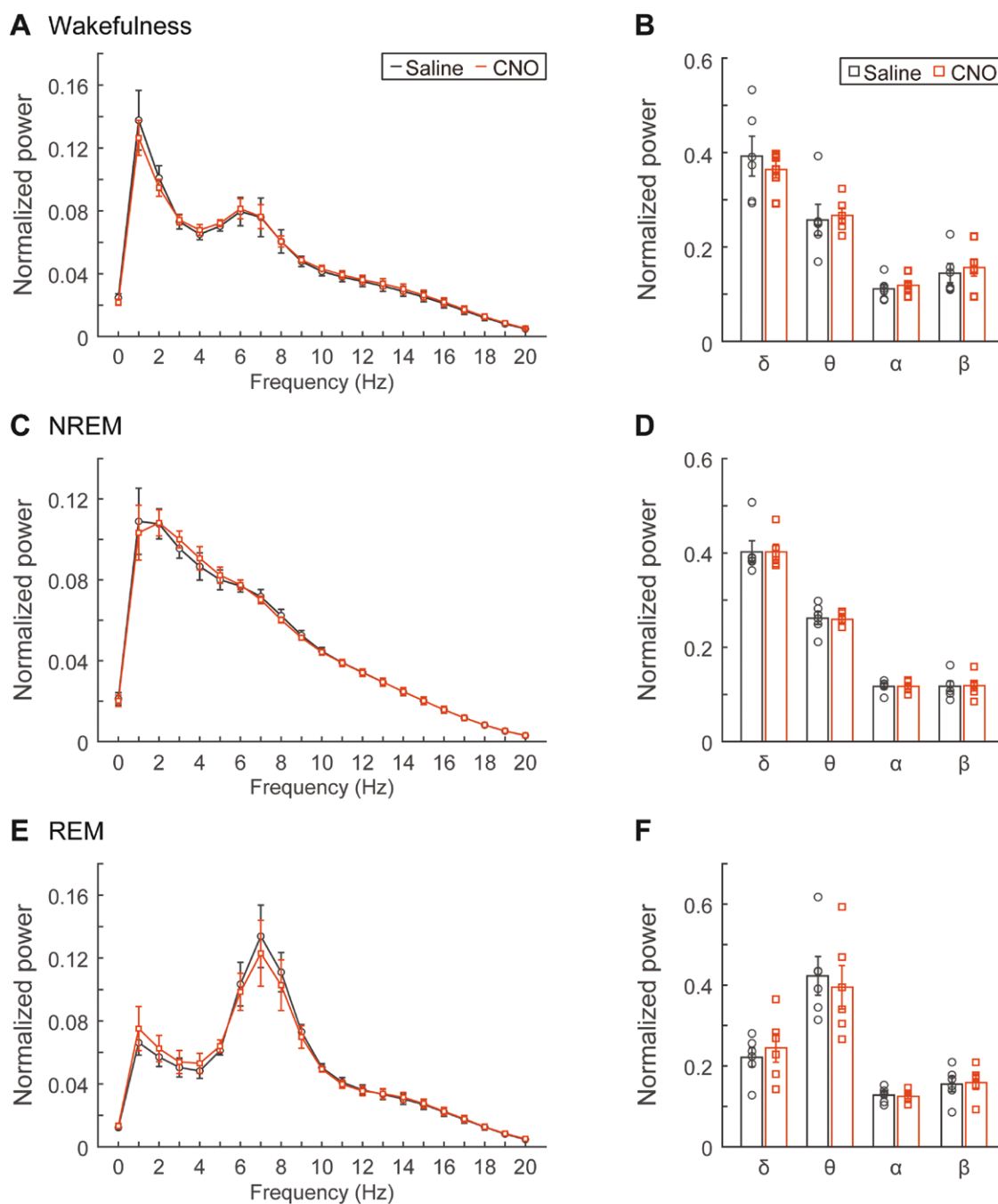


Figure 3. Effect of the chemogenetic activation of hippocampal astrocytes on EEG during sleep-wakefulness states. (A, C, and E) Average normalized EEG power spectra during wakefulness (A), NREM sleep (C), and REM sleep (E) for the 4 hours immediately after saline or CNO (1 mg/kg) administration at ZT1. (B, D, and F) Comparison of normalized delta (1–5 Hz) power, theta (6–10 Hz) power, alpha (10–13 Hz) power, and beta (13–20 Hz) power during wakefulness (B), NREM sleep (D), and REM sleep (F). Values are represented as means \pm SEM.

hippocampus. We confirmed that mice with chemogenetic activation of their astrocytes showed significant increases in cFos expression in the pons compared with saline-treated control mice ($t(2) = 13.24, p < .01$, paired t-test; Figure 5, A and B).

To determine the physiological role of activated astrocytes in the pons and whether they have a different role in sleep-wakefulness states compared with hippocampal astrocytes, GFAP-cre mice expressing hm3Dq specifically in pons astrocytes were injected i.p. with CNO (1 mg/kg) or with saline as a control at ZT1 ($n = 6$). Sleep-wakefulness states were recorded using freely moving mice. The hourly amounts of sleep-wakefulness states for

24 hours showed that REM sleep was strongly suppressed after CNO injection (repeated measures ANOVA with post hoc Tukey's test, ZT2: $p < .001$; ZT3: $p < .001$; Figure 5K and Supplementary Table S3), whereas there was no significant change in wakefulness (Figure 5C and Supplementary Table S3). Although there was a significant effect of treatment on NREM sleep during the light phase, there were no significant post hoc differences (Figure 5G and Supplementary Table S3). The activation of pons astrocytes significantly decreased the total time of REM sleep during the 4 hours after CNO administration compared with saline-treated experiments ($t(5) = -7.09, p < .001$, paired t-test; Figure 5L). The

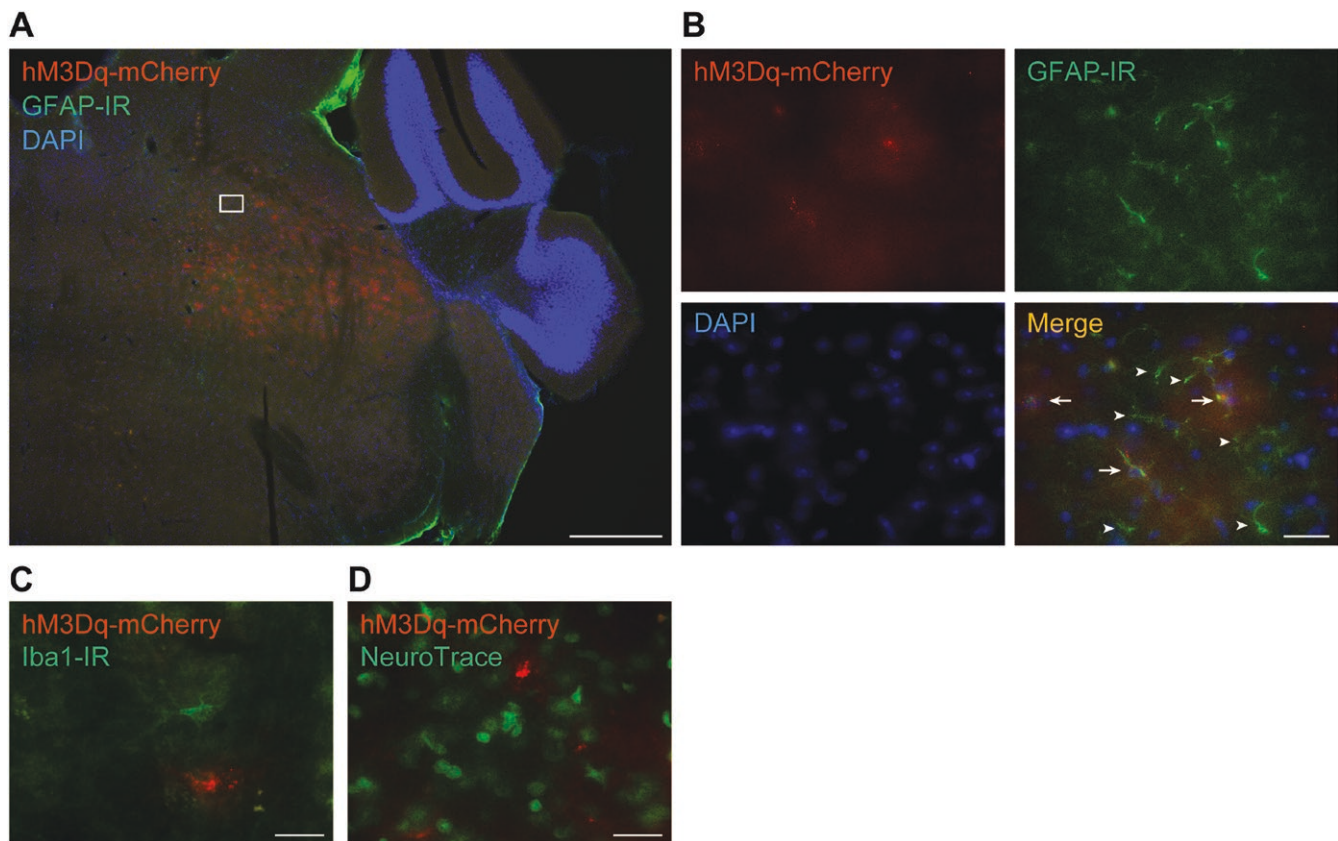


Figure 4. Specific expression of hM3Dq in astrocytes in the pons. (A) Expression pattern of hM3Dq in the pons in GFAP-cre mice. Red, hM3Dq-mCherry; green, GFAP-IR astrocytes; blue, DAPI. Scale bar: 500 μ m. (B) Higher magnification images of the square region in (A). Arrows indicate GFAP-IR astrocytes expressing hM3Dq. Arrowheads indicate GFAP-IR astrocytes not expressing hM3Dq. Scale bar: 10 μ m. (C) Fluorescence immunostaining with an anti-Iba1 antibody. Red, hM3Dq-mCherry; green, Iba1-IR microglia. Scale bar: 10 μ m. (D) NeuroTrace green fluorescent Nissl staining. Red, hM3Dq-mCherry; green, NeuroTrace green fluorescent Nissl stain-positive neurons. Scale bar: 10 μ m

total time of NREM sleep was significantly increased ($t(5) = 2.88$, $p < .05$, paired t -test; [Figure 5H](#)). On the other hand, there was no difference in the total time of wakefulness ([Figure 5D](#)). In terms of wakefulness episodes, there was no significant change in duration, but a significant reduction in number ($t(5) = -2.74$, $p < .05$, paired t -test; [Figure 5, E and F](#)). During NREM sleep, mean episode duration significantly increased ($t(5) = 4.80$, $p < .01$, paired t -test), in association with a decrease in the number of episodes ($t(5) = -2.59$, $p < .05$, paired t -test; [Figure 5, I and J](#)). In contrast, regarding REM sleep episodes, the mean duration did not change, but the number of episodes significantly decreased ($t(5) = -6.51$, $p < .01$, paired t -test; [Figure 5, M and N](#)). A significant decrease in transition frequency was observed across all sleep-wakefulness states ($t(5) = -3.34$, $p < .05$, paired t -test; [Figure 5O](#)). The transition frequency to each state was further analyzed in detail ([Figure 5P](#)). The activation of pons astrocytes via CNO injection induced a significant decrease in transition number from wakefulness to NREM sleep ($t(5) = -2.58$, $p < .05$, paired t -test), from NREM sleep to REM sleep ($t(5) = -6.36$, $p < .01$, paired t -test), and from REM sleep to wakefulness ($t(5) = -6.36$, $p < .01$, paired t -test). Taken together, these findings indicate that the activation of pons astrocytes reduces REM sleep by strongly inhibiting its onset.

Activation of pons astrocytes increases delta waves during NREM sleep

Next, to analyze the effect of the activation of pons astrocytes on the cortical oscillations during sleep-wakefulness states, a

spectral analysis of EEG was performed. EEG power was normalized as in the analysis of the activation of hippocampal astrocytes ([Figure 3](#)). Despite the results that the activation of pons astrocytes strongly suppressed REM sleep, unexpectedly, EEG power was substantially altered in NREM sleep, but not in wakefulness ([Figure 6, A and C](#) and [Supplementary Table S4](#)). Although there was a significant effect of treatment \times frequency on REM sleep, there were no significant post hoc differences ([Figure 6E](#) and [Supplementary Table S4](#)); the normalized power of EEG between 2 and 4 Hz during NREM sleep in CNO-treated experiment significantly increased compared with saline-treated experiments (repeated measures ANOVA with post hoc Tukey's test, 2 Hz: $p < .001$; 3 Hz: $p < .001$; 4 Hz: $p < .01$; [Figure 6C](#)). With respect to each frequency band, during NREM sleep, delta waves were significantly higher in CNO-treated mice than those in saline-treated mice, whereas theta, alpha, and beta waves were significantly lower (delta: $t(5) = 3.83$, $p < .05$, paired t -test; theta: $t(5) = -3.43$, $p < .05$, paired t -test; alpha: $t(5) = -4.96$, $p < .01$, paired t -test; beta: $t(5) = -5.57$, $p < .01$, paired t -test; [Figure 6D](#)). On the other hand, there were no significant differences in wakefulness and REM sleep ([Figure 6, B and F](#)). In conclusion, we demonstrated that the activation of astrocytes in the pons increases the low-frequency components in EEG during NREM sleep in mice.

Discussion

In the present study, we analyzed the sleep-wakefulness states and cortical oscillations in mice under conditions of the

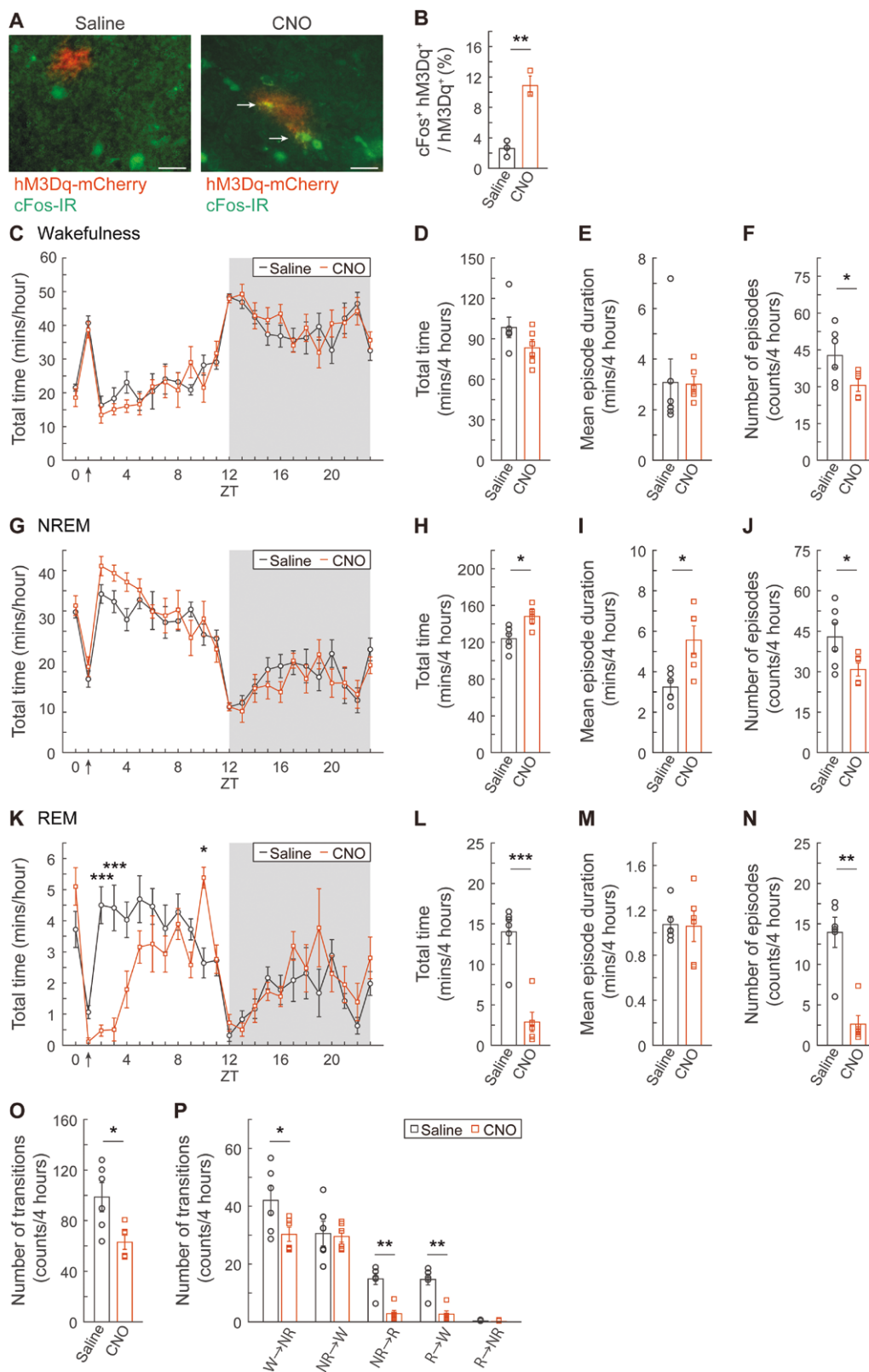


Figure 5. Effects of the chemogenetic activation of pons astrocytes on sleep-wakefulness. (A) CNO (1 mg/kg) administration to mice expressing hM3Dq in their pons astrocytes resulted in an increase in cFos expression (right) in the astrocytes (arrows) compared with saline-treated mice (left). Red, hM3Dq-mCherry; green, cFos-IR cells. Scale bar: 10 μ m. (B) Bar graph showing quantification results of c-Fos expression in the astrocytes. (C, G, and K) Hourly amounts of wakefulness (C), NREM sleep (G), and REM sleep (K) after i.p. injection of saline or CNO at ZT1 (arrows). Gray background indicates the dark period. (D, H, and L) Total amounts of wakefulness (D), NREM sleep (H), and REM sleep (L) during the 4 hours after the i.p. injection of saline or CNO. (E, I, and M) Mean episode duration of wakefulness (E), NREM sleep (I), and REM sleep (M). (F, J, and N) Number of episodes of wakefulness (F), NREM sleep (J), and REM sleep (N). (O) The number of transitions between all states during the 4 hours after saline or CNO administration. (P) The number of transitions between each sleep-wakefulness state during the 4 hours after saline or CNO administration. NR, NREM sleep; R, REM sleep; W, wakefulness. Values represent means \pm SEM; *, $p < .05$. **, $p < .01$, ***, $p < .001$.

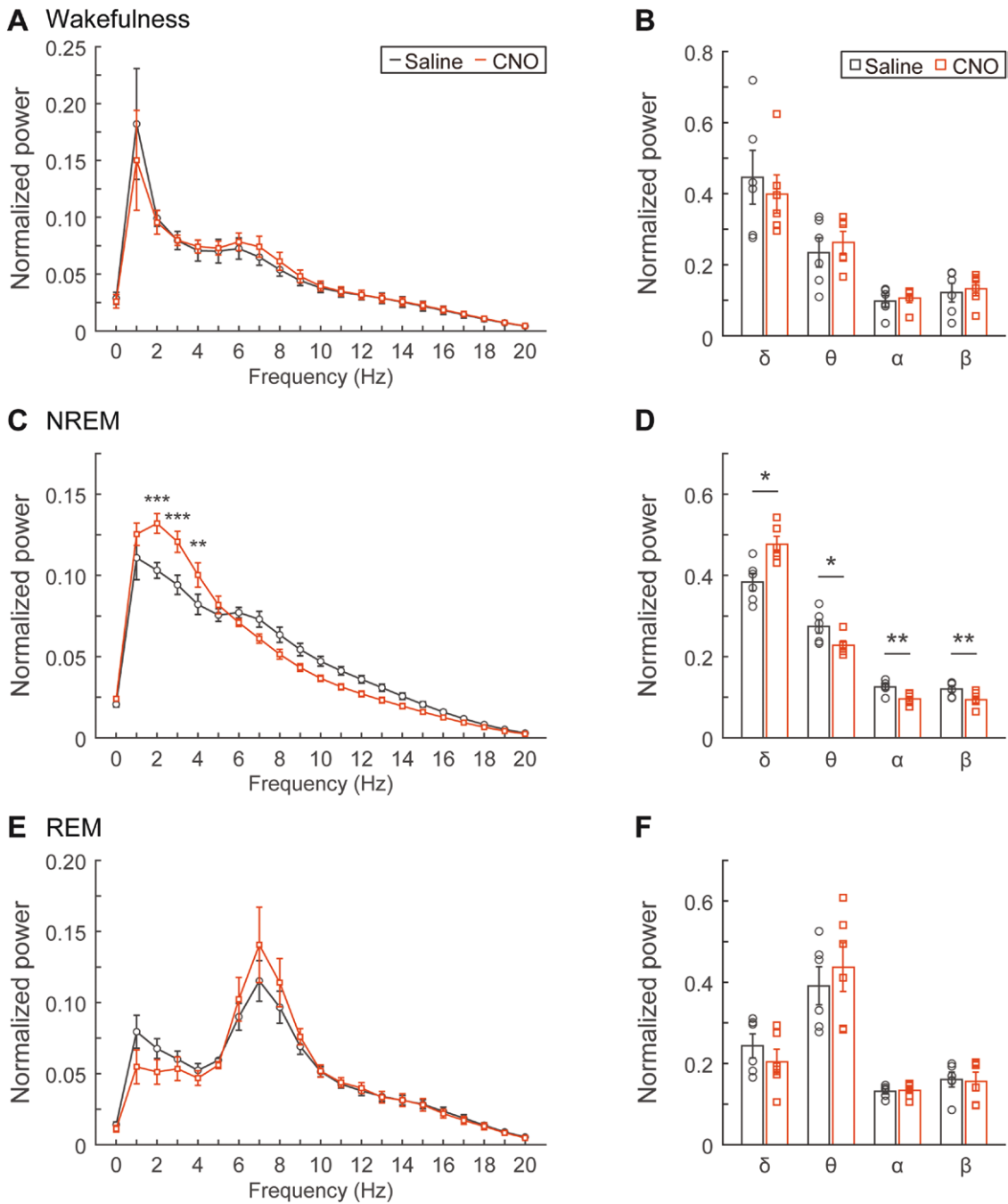


Figure 6. Effect of the chemogenetic activation of pons astrocytes on EEG during sleep-wakefulness states. (A, C, and E) Average normalized EEG power spectra during wakefulness (A), NREM sleep (C), and REM sleep (E) for 4 hours after saline or CNO (1 mg/kg) administration at ZT1. (B, D, and F) Comparison of normalized delta (1–5 Hz) power, theta (6–10 Hz) power, alpha (10–13 Hz) power, and beta (13–20 Hz) power during wakefulness (B), NREM sleep (D), and REM sleep (F). Values represent means ± SEM; *, $p < .05$. **, $p < .01$, ***, $p < .001$.

activation of hippocampal and pons astrocytes using chemogenetics. The activation of hippocampal astrocytes induced a significant decrease in the total time of wakefulness, and a significant increase in the total time of NREM sleep and REM sleep. There was little effect on cortical oscillations in any sleep-wakefulness states. On the other hand, activation of pons astrocytes substantially decreased the total time of REM sleep, accompanied by suppression of REM sleep episode occurrence. There was a significant increase in the total time of NREM sleep, but no effect on the total time of wakefulness. Moreover, the delta component during NREM sleep was significantly increased.

Activation of astrocytes modulates sleep-wakefulness states

Previous studies, including ours, demonstrated that the dynamics of intracellular Ca^{2+} concentration in astrocytes are associated with sleep-wakefulness states [9–11]. The causal association between the activity of astrocytes and sleep-wakefulness states has not been completely clarified to date, although several studies using chemogenetic techniques have been reported in the previous few years [23–26]. The use of chemogenetics ligands has considerable side effects on sleep studies; it has been reported that the administration of CNO to mice that do not express DREADD

can alter the total duration of NREM and REM sleep, as well as the number of episodes and episode duration [27, 28]. However, such side effects are observed only when CNO is administered at high doses (5 or 10 mg/kg). In a previous study using the same dose of CNO as was administered in the present study (1 mg/kg), NREM and REM sleep latency, and the episode duration of NREM sleep before REM onset were significantly affected [27]. These parameters differ from the parameters of sleep–wakefulness alterations that we demonstrated in the present study. Although our experiments lacked analysis of the direct effects of CNO on sleep–wakefulness states, it is likely that changes in sleep–wakefulness states observed here were a result of the activation of astrocytes by CNO administration, and not the CNO administration itself. This suggests that astrocytes have the ability to modulate the sleep–wakefulness state.

We compared the effects of activation of hippocampal and pons astrocytes on sleep–wakefulness states, to clarify whether there were any differences. Our results demonstrated that the activation of hippocampal astrocytes induced a moderate decrease in wakefulness and an increase in sleep. This result is inconsistent with a report that optogenetic activation of hippocampal astrocytes by expressing channelrhodopsin-2 (ChR2) does not change sleep–wakefulness states [29]. This discrepancy may be owing to differences in the experimental design between chemogenetics and optogenetics. Although astrocytes express G-protein-coupled receptors, they do not densely express large cation pores, such as ChR2 [3]. Therefore, it is likely that our present study using chemogenetics was able to activate astrocytes under conditions more similar to physiological conditions than the previous study using optogenetics. The activation of hippocampal astrocytes had little effect on the cortical oscillations during sleep–wakefulness state. However, owing to the limitation of analyzing cortical EEG only up to 20 Hz in this study, it is unclear whether frequency components, such as higher beta and gamma waves, can be altered. These points need to be investigated in the future. In contrast, the activation of pons astrocytes strongly suppressed the onset of REM sleep, resulting in a significant decrease in the total time of REM sleep. The delta component of EEG during NREM sleep was significantly increased. Despite some differences, these results were generally in agreement with those of a previous study [24]. In addition, recent studies using chemogenetics demonstrated that different brain regions affect sleep/wakefulness states in different ways. The activation of astrocytes in the basal forebrain and lateral hypothalamus increases wakefulness and decreases NREM and REM sleep [26, 30]. Furthermore, the activation of cortical astrocytes has been reported to increase sleep [23]. These results make it reasonable to assume that astrocytes contribute to sleep–wakefulness states differently depending on the brain region. Astrocytes have recently been demonstrated to be a heterogeneous population. Several types of astrocyte gene expression patterns have been identified through transcriptome analyses of various brain regions [31–34]. The heterogeneity of astrocytes may contribute to the different regulatory roles of astrocytes in the regulation of sleep–wakefulness.

Possible mechanism of modulation of sleep–wakefulness states

What are the mechanisms by which activated astrocytes modulate sleep–wakefulness states and cortical oscillations? Regarding the pons, the brain region of hM3Dq expression in astrocytes coincides with the SLD. Neurons located in the SLD are well-known to be REM-promoting neurons [35, 36]. The activity of

REM-promoting neurons in the SLD is strongly inhibited by gamma-aminobutyric acid (GABA)ergic neurons in the dorsal part of the deep mesencephalic nucleus during wakefulness and NREM sleep [37, 38]. It has been reported that activated astrocytes release glutamate, GABA, D-serine, adenosine triphosphate (ATP), and adenosine as gliotransmitters [39]. Astrocytes in the pons may release GABA, resulting in the suppression of REM-promoting neurons in the SLD. Another possibility to consider is the involvement of microglia. Microglia have also been implicated in sleep–wakefulness regulation, and it is well-known that they are activated during sleep deprivation [40–42]. We should consider the possibility that cytokines and reactive oxygen species released from astrocytes affect microglia, resulting in changes in sleep–wakefulness regulation.

The activation of astrocytes in the pons affected not only sleep–wakefulness states but also cortical oscillations. During NREM sleep, the delta component was significantly increased, whereas the theta, alpha, and beta components were significantly decreased. The sleep drive, i.e. sleep need or sleep pressure, is represented by an increase in slow wave activity power [43, 44]. Astrocytes regulate sleep pressure and increase delta wave components by releasing adenosine through soluble N-ethylmaleimide-sensitive factor attachment protein receptors [7, 8]. Previous reports showed that astrocyte Ca^{2+} signals express an accumulation of sleep pressure [9, 45]. Thus, an increase in intracellular Ca^{2+} concentration in astrocytes may cause increased sleep pressure and increased delta waves. There are, however, several concerns that need to be considered. First, the activation of hippocampal astrocytes did not result in a similar change in cortical oscillations. Secondly, recent optogenetics and chemogenetics studies have shown that increased intracellular Ca^{2+} concentration in the hypothalamus and basal forebrain does not increase the delta wave component during NREM sleep [24, 26, 29]. Thirdly, in the present study, we did not investigate whether activation of hM3Dq via CNO increases Ca^{2+} concentration in astrocytes. Taken together, there are presently insufficient lines of evidence to conclude whether increased astrocyte Ca^{2+} concentration leads to an increase in sleep pressure, and consequently, the delta component during NREM sleep. Further experiments are necessary to clarify this point.

The activation of hippocampal astrocytes significantly decreased the total time of wakefulness and increased the total time of sleep, but these were moderate alterations compared with those of the pons. It has been reported that the activity of hippocampal neurons changes according to sleep–wakefulness states [17, 46, 47]. However, there has been no line of evidence to date that hippocampal neurons are responsible for controlling sleep–wakefulness states. In addition, previous research has demonstrated that neurons in the brainstem are able to decode sleep and wakefulness states more adequately than those in the hippocampal region [13]. Considering these results, even though astrocytes in the hippocampus are activated and release gliotransmitters, they do not appear to have a substantial effect on sleep–wakefulness states. It should be noted that we did not analyze the properties of gliotransmitters in the present study. In addition, little effect on cortical oscillations was observed. Surprisingly, the theta component was not affected by the activation of hippocampal astrocytes, despite it being demonstrated that astrocyte Ca^{2+} concentration in the cortex affects cortical oscillations [23, 48].

Our results as well as those of previous studies clearly indicate that astrocytes are involved in the regulation of sleep–wakefulness states. However, as the activity of astrocytes was

artificially manipulated in these studies, the extent to which they contribute to behavior under physiological conditions remains unclear. In addition, further studies are required to clarify the details regarding the type of gliotransmitters that are released from astrocytes, how these gliotransmitters regulate neural activity, how they affect behavior, and whether there are sex differences.

Supplementary material

Supplementary material is available at *SLEEP Advances* online.

Funding

This work was supported in part by Precursory Research for Embryonic Science and Technology (PRESTO) (grant no.: JPMJPR1887) and Fusion Oriented Research for Disruptive Science and Technology (FOREST) (grant no.: JPMJFR2047) from Japan Science and Technology Agency (JST), Shiseido Female Research Science Grant, and The Inamori Foundation Grant to T.T.

Acknowledgments

Generous support from the FRIS CoRE, which is a shared research environment at Tohoku University, is acknowledged. We thank Professor Hiromu Tanimoto for helpful discussions, Sayuri Kobayashi for technical assistance, and Dr. Helena Akiko Popiel for the English language editing of the manuscript.

Disclosure Statement

Financial disclosure: none. Nonfinancial disclosure: none.

Author Contributions

Yuta Kurogi (Data curation [equal], Formal analysis [lead], Investigation [lead], Validation [lead], Visualization [lead], Writing—original draft [supporting]), Tomomi Sanagi (Data curation [supporting], Investigation [supporting], Methodology [supporting], Supervision [supporting], Writing—original draft [supporting]), Daisuke Ono (Investigation [supporting], Methodology [supporting], Resources [lead]), and Tomomi Tsunematsu (Conceptualization [lead], Data curation [equal], Formal analysis [supporting], Funding acquisition [lead], Investigation [supporting], Methodology [lead], Project administration [lead], Supervision [lead], Validation [supporting], Visualization [supporting], Writing—original draft [lead])

Data Availability

The data underlying this article will be shared on reasonable request to the corresponding author.

References

- Sofroniew MV, Vinters HV. Astrocytes: biology and pathology. *Acta Neuropathol.* 2010;**119**(1):7–35. doi:10.1007/s00401-009-0619-8
- Magistretti PJ, Allaman I. Lactate in the brain: from metabolic end-product to signalling molecule. *Nat Rev Neurosci.* 2018;**19**(4):235–249. doi:10.1038/nrn.2018.19
- Ingiosi AM, Frank MG. Goodnight, astrocyte: waking up to astroglial mechanisms in sleep. *FEBS J.* 2023;**290**(10):2553–2564. doi:10.1111/febs.16424
- Tobler I, Borbely AA, Schwyzer M, Fontana A. Interleukin-1 derived from astrocytes enhances slow wave activity in sleep EEG of the rat. *Eur J Pharmacol.* 1984;**104**(1-2):191–192. doi:10.1016/0014-2999(84)90391-1
- Scharbarg E, Walter A, Lecoin L, et al. Prostaglandin D(2) controls local blood flow and sleep-promoting neurons in the VLPO via astrocyte-derived adenosine. *ACS Chem Neurosci.* 2023;**14**(6):1063–1070. doi:10.1021/acscchemneuro.2c00660
- Faraguna U, Vyazovskiy VV, Nelson AB, Tononi G, Cirelli C. A causal role for brain-derived neurotrophic factor in the homeostatic regulation of sleep. *J Neurosci.* 2008;**28**(15):4088–4095. doi:10.1523/JNEUROSCI.5510-07.2008
- Halassa MM, Florian C, Fellin T, et al. Astrocytic modulation of sleep homeostasis and cognitive consequences of sleep loss. *Neuron.* 2009;**61**:213–219. doi:10.1016/j.neuron.2008.11.024
- Florian C, Vecsey CG, Halassa MM, Haydon PG, Abel T. Astrocyte-derived adenosine and A1 receptor activity contribute to sleep loss-induced deficits in hippocampal synaptic plasticity and memory in mice. *J Neurosci.* 2011;**31**:6956–6962. doi:10.1523/JNEUROSCI.5761-10.2011
- Ingiosi AM, Hayworth CR, Harvey DO, et al. A role for astroglial calcium in mammalian sleep and sleep regulation. *Curr Biol.* 2020;**30**:4373–4383.e7. doi:10.1016/j.cub.2020.08.052
- Bojarskaite L, Bjornstad DM, Pettersen KH, et al. Astrocytic Ca(2+) signaling is reduced during sleep and is involved in the regulation of slow wave sleep. *Nat Commun.* 2020;**11**(1):3240. doi:10.1038/s41467-020-17062-2
- Tsunematsu T, Sakata S, Sanagi T, Tanaka KF, Matsui K. Region-specific and state-dependent astrocyte Ca(2+) dynamics during the sleep-wake cycle in mice. *J Neurosci.* 2021;**41**(25):5440–5452. doi:10.1523/JNEUROSCI.2912-20.2021
- Foley J, Blutstein T, Lee S, Erneux C, Halassa MM, Haydon P. Astrocytic IP3/Ca2+ signaling modulates theta rhythm and REM sleep. *Front Neural Circuits.* 2017;**11**:1–11.
- Tsunematsu T, Patel AA, Onken A, Sakata S. State-dependent brainstem ensemble dynamics and their interactions with hippocampus across sleep states. *Elife.* 2020;**9**:e52244. doi:10.7554/eLife.52244
- Sulaman BA, Wang S, Tyan J, Eban-Rothschild A. Neuro-orchestration of sleep and wakefulness. *Nat Neurosci.* 2023;**26**(2):196–212. doi:10.1038/s41593-022-01236-w
- Scammell TE, Arrigoni E, Lipton JO. Neural circuitry of wakefulness and sleep. *Neuron.* 2017;**93**:747–765. doi:10.1016/j.neuron.2017.01.014
- Nunez A, Buno W. The theta rhythm of the hippocampus: from neuronal and circuit mechanisms to behavior. *Front Cell Neurosci.* 2021;**15**:649262. doi:10.3389/fncel.2021.649262
- Buzsáki G. Theta oscillations in the hippocampus review. *Cell.* 2002;**33**:325–340.
- Koehl M, Battle S, Meerlo P. Sex differences in sleep: the response to sleep deprivation and restraint stress in mice. *Sleep.* 2006;**29**(9):1224–1231. doi:10.1093/sleep/29.9.1224
- Mieda M, Ono D, Hasegawa E, et al. Cellular clocks in AVP neurons of the SCN are critical for interneuronal coupling regulating circadian behavior rhythm. *Neuron.* 2015;**85**(5):1103–1116. doi:10.1016/j.neuron.2015.02.005
- Tobler I, Deboer T, Fischer M. Sleep and sleep regulation in normal and prion protein-deficient mice. *J Neurosci.* 1997;**17**:1869–1879. doi:10.1523/JNEUROSCI.17-05-01869.1997

21. Radulovacki M, Virus RM, Djuricic-Nedelson M, Green RD. Adenosine analogs and sleep in rats. *J Pharmacol Exp Ther*. 1984;**228**(2):268–274.
22. Pendergast JS, Tuesta LM, Bethea JR. Oestrogen receptor beta contributes to the transient sex difference in tyrosine hydroxylase expression in the mouse locus coeruleus. *J Neuroendocrinol*. 2008;**20**(10):1155–1164. doi:[10.1111/j.1365-2826.2008.01776.x](https://doi.org/10.1111/j.1365-2826.2008.01776.x)
23. Vaidyanathan TV, Collard M, Yokoyama S, Reitman ME, Poskanzer KE. Cortical astrocytes independently regulate sleep depth and duration via separate GPCR pathways. *Elife*. 2021;**10**:e63329. doi:[10.7554/eLife.63329](https://doi.org/10.7554/eLife.63329)
24. Peng W, Liu X, Ma G, et al. Adenosine-independent regulation of the sleep-wake cycle by astrocyte activity. *Cell Discov*. 2023;**9**(1):16. doi:[10.1038/s41421-022-00498-9](https://doi.org/10.1038/s41421-022-00498-9)
25. Liu PC, Yao W, Chen XY, et al. Parabrachial nucleus astrocytes regulate wakefulness and isoflurane anesthesia in mice. *Front Pharmacol*. 2022;**13**:991238. doi:[10.3389/fphar.2022.991238](https://doi.org/10.3389/fphar.2022.991238)
26. Ingiosi AM, Hayworth CR, Frank MG. Activation of basal forebrain astrocytes induces wakefulness without compensatory changes in sleep drive. *J Neurosci*. 2023;**43**(32):5792–5809. doi:[10.1523/JNEUROSCI.0163-23.2023](https://doi.org/10.1523/JNEUROSCI.0163-23.2023)
27. Traut J, Mengual JP, Meijer EJ, et al. Effects of clozapine-N-oxide and compound 21 on sleep in laboratory mice. *Elife*. 2023;**12**:e84740. doi:[10.7554/eLife.84740](https://doi.org/10.7554/eLife.84740)
28. Gomez JL, Bonaventura J, Lesniak W, et al. Chemogenetics revealed: DREADD occupancy and activation via converted clozapine. *Science*. 2017;**357**(6350):503–507. doi:[10.1126/science.aan2475](https://doi.org/10.1126/science.aan2475)
29. Kim JH, Choi IS, Jeong JY, Jang IS, Lee MG, Suk K. Astrocytes in the ventrolateral preoptic area promote sleep. *J Neurosci*. 2020;**40**(47):8994–9011. doi:[10.1523/JNEUROSCI.1486-20.2020](https://doi.org/10.1523/JNEUROSCI.1486-20.2020)
30. Cai P, Huang SN, Lin ZH, et al. Regulation of wakefulness by astrocytes in the lateral hypothalamus. *Neuropharmacology*. 2022;**221**:109275. doi:[10.1016/j.neuropharm.2022.109275](https://doi.org/10.1016/j.neuropharm.2022.109275)
31. Chai H, Diaz-Castro B, Shigetomi E, et al. Neural circuit-specialized astrocytes: transcriptomic, proteomic, morphological, and functional evidence. *Neuron*. 2017;**95**(3):531–549.e9. doi:[10.1016/j.neuron.2017.06.029](https://doi.org/10.1016/j.neuron.2017.06.029)
32. Zeisel A, Hochgerner H, Lonnerberg P, et al. Molecular architecture of the mouse nervous system. *Cell*. 2018;**174**(4):999–1014.e22. doi:[10.1016/j.cell.2018.06.021](https://doi.org/10.1016/j.cell.2018.06.021)
33. Batiuk MY, Martirosyan A, Wahis J, et al. Identification of region-specific astrocyte subtypes at single cell resolution. *Nat Commun*. 2020;**11**(1):1220. doi:[10.1038/s41467-019-14198-8](https://doi.org/10.1038/s41467-019-14198-8)
34. Bayraktar OA, Bartels T, Holmqvist S, et al. Astrocyte layers in the mammalian cerebral cortex revealed by a single-cell in situ transcriptomic map. *Nat Neurosci*. 2020;**23**(4):500–509. doi:[10.1038/s41593-020-0602-1](https://doi.org/10.1038/s41593-020-0602-1)
35. Luppi PH, Chancel A, Malcey J, Cabrera S, Fort P, Maciél RM. Which structure generates paradoxical (REM) sleep: the brainstem, the hypothalamus, the amygdala or the cortex? *Sleep Med Rev*. 2024;**74**:101907. doi:[10.1016/j.smrv.2024.101907](https://doi.org/10.1016/j.smrv.2024.101907)
36. Clement O, Sapin E, Berod A, Fort P, Luppi PH. Evidence that neurons of the sublaterodorsal tegmental nucleus triggering paradoxical (REM) sleep are glutamatergic. *Sleep*. 2011;**34**(4):419–423. doi:[10.1093/sleep/34.4.419](https://doi.org/10.1093/sleep/34.4.419)
37. Hayashi Y, Kashiwagi M, Yasuda K, et al. Cells of a common developmental origin regulate REM / non-REM sleep and wakefulness in mice. *Science*. 2015;**350**:957–961. doi:[10.1126/science.aad1023](https://doi.org/10.1126/science.aad1023)
38. Chen ZK, Dong H, Liu CW, et al. A cluster of mesopontine GABAergic neurons suppresses REM sleep and curbs cataplexy. *Cell Discov*. 2022;**8**(1):115. doi:[10.1038/s41421-022-00456-5](https://doi.org/10.1038/s41421-022-00456-5)
39. Savtchouk I, Volterra A. Gliotransmission: beyond Black-and-White. *J Neurosci*. 2018;**38**(1):14–25. doi:[10.1523/JNEUROSCI.0017-17.2017](https://doi.org/10.1523/JNEUROSCI.0017-17.2017)
40. Ma C, Li B, Silverman D, et al. Microglia regulate sleep through calcium-dependent modulation of norepinephrine transmission. *Nat Neurosci*. 2024;**27**(2):249–258. doi:[10.1038/s41593-023-01548-5](https://doi.org/10.1038/s41593-023-01548-5)
41. Wadhwa M, Kumari P, Chauhan G, et al. Sleep deprivation induces spatial memory impairment by altered hippocampus neuroinflammatory responses and glial cells activation in rats. *J Neuroimmunol*. 2017;**312**:38–48. doi:[10.1016/j.jneuroim.2017.09.003](https://doi.org/10.1016/j.jneuroim.2017.09.003)
42. Bellesi M, de Vivo L, Chini M, Gilli F, Tononi G, Cirelli C. Sleep loss promotes astrocytic phagocytosis and microglial activation in mouse cerebral cortex. *J Neurosci*. 2017;**37**(21):5263–5273. doi:[10.1523/JNEUROSCI.3981-16.2017](https://doi.org/10.1523/JNEUROSCI.3981-16.2017)
43. Tobler I, Borbely AA. The effect of 3-h and 6-h sleep deprivation on sleep and EEG spectra of the rat. *Behav Brain Res*. 1990;**36**(1-2):73–78. doi:[10.1016/0166-4328\(90\)90161-7](https://doi.org/10.1016/0166-4328(90)90161-7)
44. Franken P, Chollet D, Tafti M. The homeostatic regulation of sleep need is under genetic control. *J Neurosci*. 2001;**21**(8):2610–2621. doi:[10.1523/JNEUROSCI.21-08-02610.2001](https://doi.org/10.1523/JNEUROSCI.21-08-02610.2001)
45. Blum ID, Keles MF, Baz ES, et al. Astroglial calcium signaling encodes sleep need in drosophila. *Curr Biol*. 2021;**31**(1):150–162.e7. doi:[10.1016/j.cub.2020.10.012](https://doi.org/10.1016/j.cub.2020.10.012)
46. Grosmark AD, Mizuseki K, Pastalkova E, Diba K, Buzsáki G. REM sleep reorganizes hippocampal excitability. *Neuron*. 2012;**75**:1001–1007. doi:[10.1016/j.neuron.2012.08.015](https://doi.org/10.1016/j.neuron.2012.08.015)
47. Buzsáki G. Hippocampal sharp wave-ripple: a cognitive biomarker for episodic memory and planning. *Hippocampus*. 2015;**25**(10):1073–1188. doi:[10.1002/hipo.22488](https://doi.org/10.1002/hipo.22488)
48. Poskanzer KE, Yuste R. Astrocytes regulate cortical state switching in vivo. *Proc Natl Acad Sci USA*. 2016;**113**:1–10.